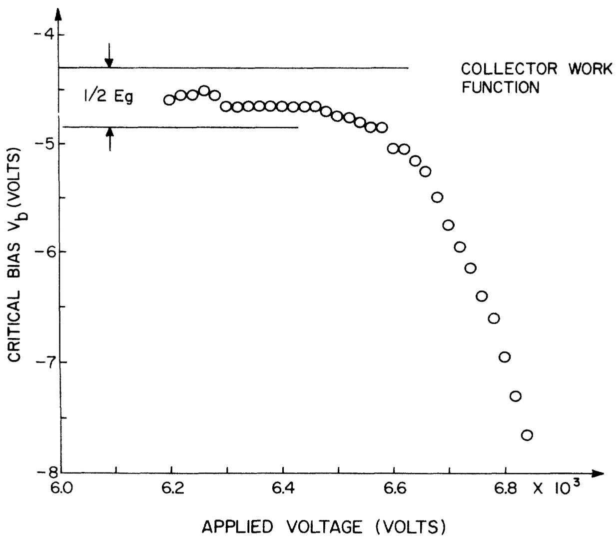

FIG. 3. Critical bias measured as a function of applied voltage for a silicon emitter. The reference voltage of 4.29 volts corresponding to emission from the Fermi level is shown as a horizontal line.

The energy of the electrons is below the Fermi energy by an amount which is less than one half the band gap for silicon. This is in keeping with the fact that silicon is known to develop a strong *p*-type surface due to boron contamination when heated in a Pyrex vacuum system.[7]

The possibility that the observed decrease in energy at higher fields is due to the penetration of the electric field into the silicon must be ruled out. Had this been the case, the bottom of the conduction band would have been depressed below the Fermi level when an energy decrease of about 0.85 volts occurred. This, in turn, would have given rise to strong emission at the Fermi level which would have been observed at a bias of 4.29 volts as in the case of a metal emitter.

The additional negative bias required at higher fields is believed to be due to an increase in the potential difference across the silicon emitter itself. As the applied potential at the anode is increased, the exponential rise in emission current causes a corresponding increase in the *IR* drop across the emitter. The apex of the emitter, therefore, becomes more positive with respect to the collector; this in turn requires a more negative tip bias for the onset of current at the collector. This emphasizes the need to restrict measurements of critical bias to those values which are not sensitive to the high voltage applied to the anode.

Techniques are being developed in field emission which will make it possible to prepare samples of semiconductors with clean surfaces which can be used for critical bias measurements. These can be expected to contribute to an understanding of the nature of the surface of semiconductors.

The author would like to thank Professor Joseph Callaway and Professor A. W. Lawson for suggestions relating to this work.

[1]F. G. Allen, J. Phys. Chem. Solids 8, 119 (1959).
[2]M. I. Elinson and G. F. Vasil'ev, Radiotekh. i Elektron. 4, 728 (1959).
[3]T. Fischer, Helv. Phys. Acta 33, 961 (1960).
[4]R. L. Perry, J. Appl. Phys. 33, 1875 (1962).
[5]R. Stratton, Phys. Rev. 125, 67 (1962).
[6]R. D. Young and E. W. Müller, Phys. Rev. 113, 115 (1959).
[7]J. T. Law, J. Phys. Chem Solids 14, 9 (1960).

EFFECT OF PLASTIC DEFORMATION ON NEUTRON IRRADIATION DAMAGE IN COPPER AND ALUMINUM AT 1.8°K

M. L. Swanson, G. R. Piercy, and D. J. Mackinnon
Atomic Energy of Canada Limited, Chalk River, Ontario, Canada
(Received October 12, 1962)

Focusing collisions[1] in close-packed lattices have been used to interpret many irradiation effects. In particular, the enhanced damage rate observed[2] for reactor-irradiated plastically deformed Cu has been explained by the defocusing of focusons at stacking faults.[3] It was shown that extended dislocations could cause an increase of as much as 50% in the damage rate of Cu. This was in rough agreement with the experimental results of Blewitt,[2] which showed a 10% enhancement for Cu deformed to fracture, and a 30% enhancement for Cu deformed with twinning at 4.2°K. It was expected[3] that a metal such as Al, with ionic diameter considerably smaller than the interatomic distance (an open lattice) and with a high stacking fault energy,[4] would exhibit little change in damage rate as a result of deformation. Thus the validity of the focusing collision model could indirectly be checked by irradiation of various annealed and deformed metals. The results to be reported here on the neutron irradiation of annealed and cold-worked Cu and Al constitute part of such an irradiation program.

The samples were prepared by rolling annealed 0.010-in. high-purity Cu and Al wires at room temperature to 0.003 in. and winding the strips on alumina rods. Some samples were then again annealed and others were kept in liquid nitrogen to reduce defect annihilation. The metals were irradiated in a fission neutron flux of 5.5×10^8 n/cm^2 sec in the D-3 external-beam liquid helium cryostat[5] of the NRU reactor. (The flux was determined by means of sulfur threshold detectors.) Each sample received the same neutron flux within the experimental flux measurement error of 3%. The irradiation damage was determined by measuring electrical resistivities in situ using a current of 1 ampere in a potentiometric circuit; the sensitivity was 2×10^{-13} ohm cm. The samples were always immersed in liquid He II at a temperature of 1.8°K, which was controlled to ±0.001K° by means of a 150-ohm Allen-Bradley carbon resistance thermometer. The thermometer, periodically checked by helium vapor pressure measurements, was found to be very stable during irradiations of at least five days; insignificant calibration changes were required after cycling to room temperature. The samples were annealed after irradiation at approximately 80°K by allowing the cryostat to warm to the liquid nitrogen jacket temperature.

The results are summarized in Table I and are plotted in Fig. 1, where the resistivity increment caused by irradiation is plotted as a function of the integrated fission neutron flux. All damage rates were accurately linear. The damage rate of deformed copper was approximately 10% greater than that of annealed copper, in agreement with the results of Blewitt.[2] The effect of deformation was, surprisingly, much greater for Al; the enhancement was 32.2% for a sample having a residual resistivity in the annealed condition of $\rho_0 = 2.00\times10^{-9}$ ohm cm (Fig. 1). This result has been supported by several experiments using aluminum of different purity, thickness, and degree of deformation (Table I). The enhancement was

Table I. Irradiation damage in annealed and deformed Cu and Al at 1.8°K.

Sample[a]		Residual resistivity, ρ_0 (10^{-9} ohm cm)	Damage rate [10^{-25} ohm cm/(n/cm^2)]	Enhancement	Recovery to 80°K
			Copper		
1.	Annealed	2.58	1.00		35%
	Deformed[b]	22.4	1.07	7%	42%
2.	Annealed	3.80	0.95		
	Deformed	21	1.06	12%	
			Aluminum		
1.	Annealed	3.76	2.66		54%
	Deformed	12.0	3.35	26%	64%
2.	(a) Annealed	2.00	2.51		59%
	Deformed	7.30	3.32	32.2%	63%
	(b) Annealed	2.00	2.54		58%
	Deformed	5.22	3.18	25%	62%
3.	Annealed	1.75	2.51		54%
	4% Deformed	6.10	3.21	28.1%	61%
	8% Deformed	6.39	3.43	36.6%	61%
	12% Deformed	7.11	3.42	36.4%	62%
4.	Annealed	1.49	2.60		55%
	Deformed	6.13	3.61	39%	66%

[a]All samples were 99.999% purity, with the exception of Al No. 1, which was 99.99%. All samples were 0.003-in. strip with the exception of Al No. 4, which was 0.008-in. strip.

[b]All unspecified deformations were 12% reduction in area.

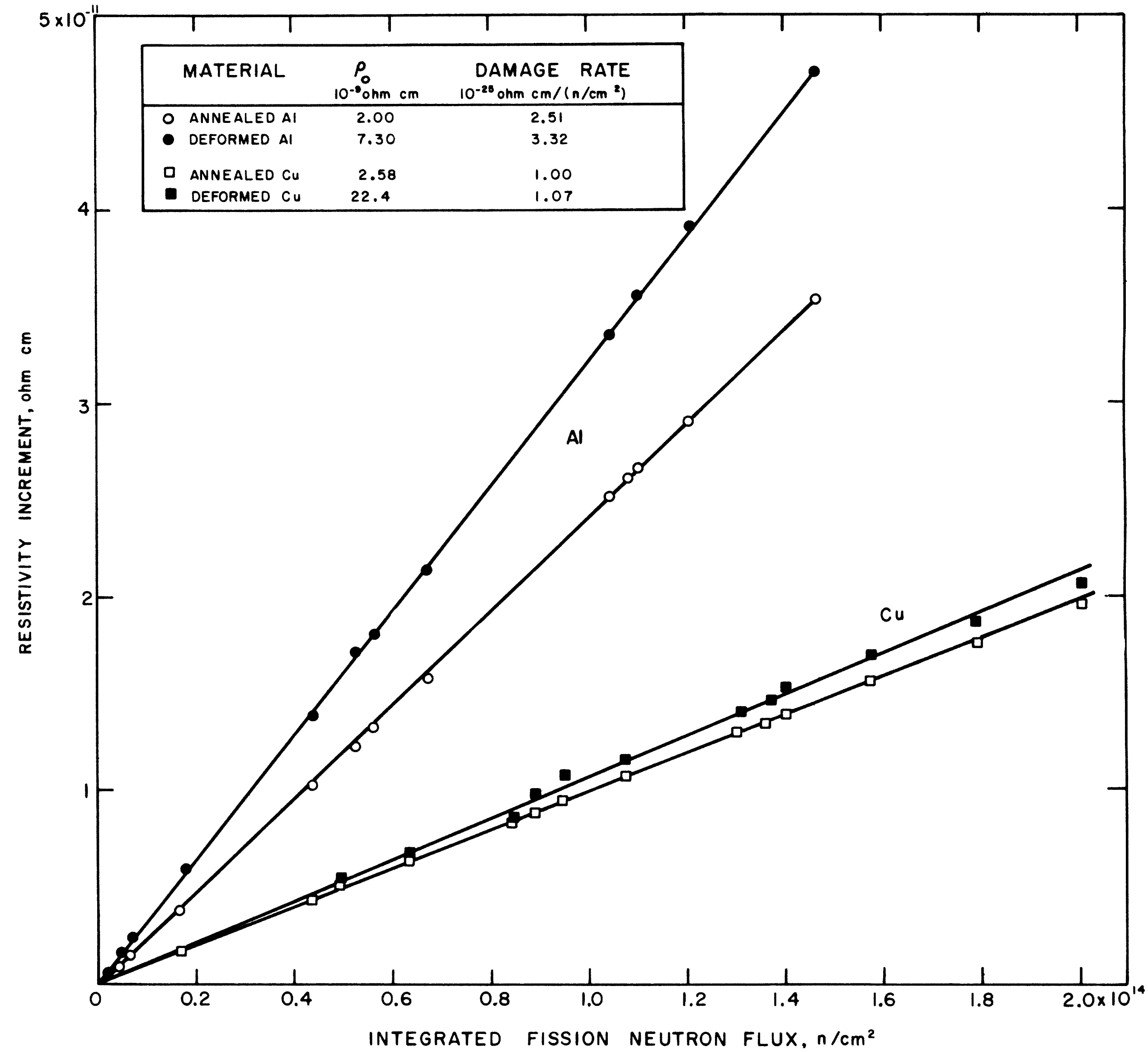

FIG. 1. Neutron irradiation damage in annealed and deformed aluminum and copper.

relatively insensitive to deformations of more than 4 % reduction in area (Sample 3, Table I). Prolonged annealing at room temperature after deformation reduced the enhancement to approximately 25 % [Sample 2(b) in Table I]. Increasingly pure samples exhibited greater enhancements, although the damage rates of the annealed samples were identical within experimental error. Corrections for the size effect have not been included in these results; calculations based on Sondheimer's formulas[6] show that the resultant error in damage rate is less than 2 %. Further experiments with varying impurity content and dislocation density of Al are planned.

The observed recovery of annealed Cu and Al to 80°K was in agreement with results of previous investigators.[7] It is interesting to note that the recovery of deformed samples was in each case slightly greater than that of annealed ones.

This unexpected enhancement of neutron irradiation damage for deformed Al indicates that long-range transfer of energy is important in irradiated Al. It is difficult to attribute this energy transfer to focusing collisions in the open lattice of Al, but a possible alternative is the recently proposed tunnel focusing,[8] whereby knock-on atoms can be focused between close-packed rows of atoms for large distances. Since this focusing is not limited by the knock-on energy, it might be very important in aluminum.

[1]R. H. Silsbee, J. Appl. Phys. 28, 1246 (1957).
[2]T. H. Blewitt et al., Bull. Am. Phys. Soc. 4, 135 (1959); Oak Ridge National Laboratory Report No. 2614, 1958 (unpublished), p. 67.
[3]G. Leibfried, J. Appl. Phys. 31, 117 (1960).
[4]A. Seeger, Defects in Crystalline Solids (The Physical Society, London, England, 1955), p. 328.
[5]D. J. Mackinnon and G. R. Piercy, Atomic Energy of Canada Limited Report No. 1423, 1961 (unpublished).
[6]E. H. Sondheimer, Advances in Physics 1, 1 (1952).
[7]T. H. Blewitt et al., Oak Ridge National Laboratory Report No. 3017, 1960 (unpublished), p. 28.
[8]M. T. Robinson, D. K. Holmes, and O. S. Oen, Bull. Am. Phys. Soc. 7, 171 (1962).

DOPPLER-SHIFTED CYCLOTRON RESONANCE AND ALFVEN WAVE DAMPING IN BISMUTH

Jordan Kirsch
Watson Scientific Computing Laboratory, International Business Machines Corporation, New York, New York

and

P. B. Miller
Thomas J. Watson Research Center, International Business Machines Corporation, Yorktown Heights, New York
(Received October 12, 1962)

At large magnetic fields the transmission of microwaves through bismuth is essentially undamped and can be regarded as Alfvén waves in a solid-state plasma.[1] We have observed a large kink in the 9-kMc/sec microwave absorption of bismuth as a perpendicularly applied magnetic field was varied through 1500 gauss. These experiments have been performed at 2°K with the field parallel to the binary axis. The kink has been identified as a Doppler-shifted cyclotron resonance whose position is approximately given by

$$\omega_c = \omega + v_{0z} k_A, \qquad (1)$$

where v_{0z} is the maximum velocity component along the magnetic field H of a carrier at the Fermi surface, k_A is the Alfvén wave vector of the microwave field in the metal, and ω_c is the cyclotron frequency. For an isotropic plasma the Alfvén wave vector is given by[1]

$$k_A = (\omega/H)(4\pi \sum_j n_j m_j)^{1/2}, \qquad (2)$$

where n_j is the density of the jth plasma carrier, m_j its mass, and the summation extends over all carriers. Equations (1) and (2) may be simply extended to the case in which each carrier is an ellipsoid of revolution about the field direction by the substitution of the cyclotron effective mass for m_j. In this model the Fermi velocity is determined by the mass component in the binary direction and the Fermi energy. Any damping of the electromagnetic wave corresponding to real transitions between Landau levels can only take place if the condition given by (1) arising from a selection rule can be satisfied for some carrier on the Fermi surface whose velocity along H is $v_z \leq v_{0z}$.[2] It is clear from Eqs. (1) and (2) that at large H the equality (1) is not satisfied; hence the Alfvén waves are undamped. As H is lowered it finally reaches a value H_c where Eq. (1) becomes an equality for the carrier with $v_z = v_{0z}$ and real transitions between Landau levels take place. The real transitions at H_c cause strong damping of the Alfvén waves and the appearance of a Doppler-shifted resonance in the surface resistance R.

A plot of the observed surface resistance is shown in Fig. 1. The Doppler-shifted kink appears at 1500 gauss. The proportionality of R to H above the kink corresponds to the existence of undamped Alfvén waves whose wave vector is given by Eq. (2).[1] The peak at 125 gauss corresponds to the dielectric anomaly previously observed by Galt et al.[3] The kink field is larger by a factor of about two than that predicted by the normal cyclotron resonance condition $\omega = \omega_c$ using the largest reported cyclotron mass ($0.25\, m_0$).[3] The observed frequency variation of the kink field H_c is plotted in Fig. 2. H_c is not proportional to ω since it does not extrapolate through the origin, and hence does not correspond to the normal cyclotron resonant condition $\omega = \omega_c$. In Fig. 2 we have also plotted the variation of H_c given by Eq. (1) for the holes, using the mass tensor and Fermi energy given by Jain and Koenig.[4] It is evident that there is satisfactory agreement with the experimental points.